water

MDPI

Article

Stable Isotope Reveals Tap Water Source under Different Water Supply Modes in the Eastern Margin of the Qinghai–Tibet Plateau

Mingxia Du, Mingjun Zhang *, Shengjie Wang, Hongfei Meng, Cunwei Che and Rong Guo

College of Geography and Environmental Science, Northwest Normal University, Lanzhou 730070, China; mingxiadu@126.com (M.D.); geowang@126.com (S.W.); mhf824061@163.com (H.M.); geoche2017@126.com (C.C.); gsgrong@163.com (R.G.)

* Correspondence: mjzhang2004@163.com; Tel.: +86-0931-797-1750

Received: 7 October 2019; Accepted: 4 December 2019; Published: 6 December 2019

Abstract: Based on 1260 tap water samples gathered monthly and 136 surface water samples collected seasonally in the eastern margin of the Qinghai–Tibet Plateau, the local tap water line, the basic spatiotemporal characteristics of tap water isotopes, and their indication for water source under different water supply modes were discussed, linking the local tap water supply and water source information. A new tap water isotopes data set based on dense sampling sites was established, which was reliable for the analysis of tap water isotope features, tap water supply management, and tap water sources. The main conclusions are: (1) The local tap water lines in Gannan and Longnan are $\delta^2H = (7.06 \pm 0.17)\ \delta^{18}O + (3.24 \pm 1.75)$ ($r^2 = 0.81$, $p < 0.01$) and $\delta^2H = (5.66 \pm 0.09)\ \delta^{18}O + (-8.12 \pm 0.82)$ ($r^2 = 0.82$, $p < 0.01$), respectively. (2) The annual mean δ^2H and $\delta^{18}O$ in tap water show an increasing trend from southwest to northeast. The seasonal differences of δ^2H and $\delta^{18}O$ in tap water in Gannan and Longnan are small. (3) The correlation of tap water isotopes with those in main source water is high, while that of isotopes in tap water with those in non-water source is low. Under the central water supply mode by local tap water company, tap water isotopes in Gannan where groundwater is the direct water source show weak connection with those in surface water and precipitation, and those in tap water in Longnan with surface water as main source water reveal good connection with isotopes in surface water. Under mixed water supply modes, tap water isotopes indicate that surface water is the main tap water source in Gannan and Longnan with multiple water sources.

Keywords: δ^2H and $\delta^{18}O$; tap water; surface water; water source; Qinghai–Tibet Plateau

1. Introduction

Tap water isotopes are well proven to be essential indicators [1–10] for studies in many fields [10–22], including hydrology, ecology, climatology, forensic, and so on. With the development of isotope methods, isotopes have been gradually applied to tap water research [23–32]. At present, studies on isotopes in tap water [33,34] throughout the world are relatively few. Their study areas have mainly involved the United States of America (e.g., the San Francisco Bay Area [31], the Salt Lake Valley of northern Utah [30], western and the whole United States [35–37]), South Africa [30], and China [34,38]. The main research contents include basic features (e.g., spatial and temporal variations, local tap water line) of tap water isotopes, tap water source, the applicability of tap water to relevant fields, and so on. These studies have enriched the knowledge of tap water isotope features, tap water supply mode and management strategy of local water resources.

At present, studies of tap water isotopes in China can be seldom found, except for reports on isotopes in tap water throughout China [34,38]. Features of tap water isotopes and their relationship with precipitation isotopes were exhibited. The water supply systems in China, which have a vast territory, are complex [39]. Further studies of tap water isotopes based on dense sampling sites are needed to finely explore the isotopic composition of tap water and its indication for water source, especially in areas with multiple water supply modes.

In southern Gansu Province, eastern margin of Qinghai–Tibet Plateau, different water supply modes, including central water supply (e.g., supplied by rural drinking water safety project, supplied by tap water company) and decentralized water supply, coexist in the Gannan Tibetan Autonomous Prefecture (Gannan) and Longnan. In the existing studies in China [34,38,40], only four tap water sampling points were involved in Gannan and Longnan, which cannot accurately reflect the local tap water isotope landscape, seasonal differences, and the significance of water source indication. In this study, isotopes in 1396 water samples (tap water samples: 1260; surface water samples: 136) were analyzed, and the local tap water line, the basic spatiotemporal characteristics of isotopes, and indication for water source under different water supply modes were discussed, combining the field survey data about water supply and sources. This research is beneficial for understanding tap water isotopes, water supply, and water source determination.

2. Study Area

Areas analyzed in this study were located in southern Gansu, including the Gannan Tibetan Autonomous Prefecture (Gannan) and Longnan (Figure 1). Gannan is one of the ten Tibetan Autonomous Prefectures in China and located between 100°46′–104°44′ E and 33°06′–36°10′ N, with an area of 4.02×10^4 km^2. The elevation in Gannan is between 1100 and 4900 m, mainly above 3000 m. The temperature difference between day and night is large. There are more than 120 rivers or streams flowing in Gannan, such as the Yellow River, Tao River, Da Xia River, Pai-lung River, and so on. Longnan is situated between 104°01′–106°35′ E and 32°35′–34°32′ N, with an area of 2.79×10^4 km^2. Longnan is the only region in Gansu which belongs to the Yangtze River system and has a subtropical climate. High mountains, river valley, hills, and basins are interlaced in Longnan.

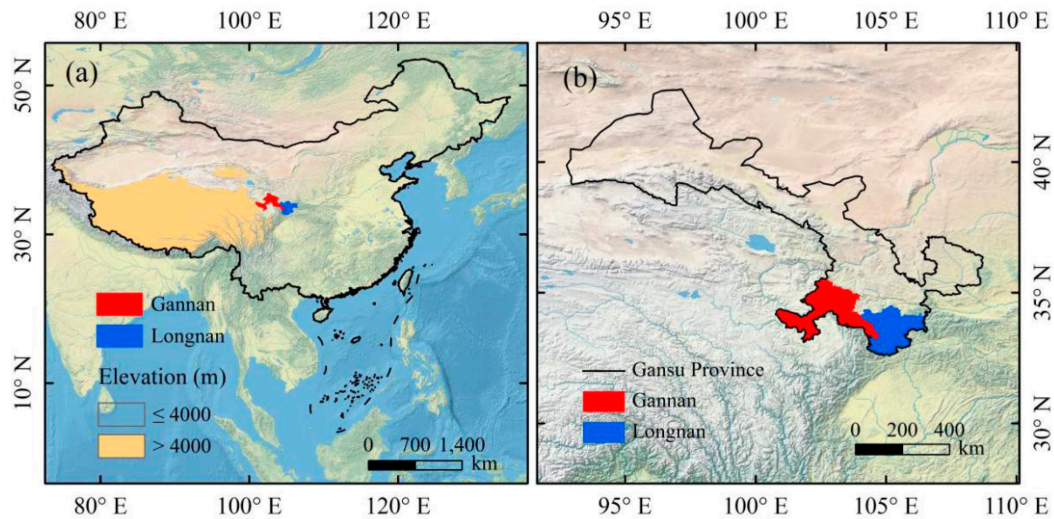

Figure 1. Study area in this study. (**a**) Location of Gannan and Longnan in China. (**b**) Location of Gannan and Longnan in Gansu Province. The satellite-derived land cover base map derived from Natural Earth (http://www.naturalearthdata.com). Spatial distribution of elevation came from Shuttle Radar Topography Mission 90M Resolution Raw Elevation Data (SRTMDEM 90M; http://www.gscloud.cn/sources/?cdataid=302&pdataid=10).

3. Data and Method

3.1. Collection of Water Samples

Surface water and tap water samples were gathered by field work of our team in southern Gansu from May 2017 to April 2018. Cold tap water was collected into bottles after running the tap for 10 s [41]. Fresh surface water was collected from rivers, streams, or mountain springs flowing in southern Gansu. Tap water samples were gathered monthly from May 2017 to April 2018 (except for June 2017). Surface water samples were collected 5 times seasonally between May 2017 and April 2018 (in May 2017, July 2017, October 2017, January 2018, and April 2018). Sampling sites had relatively complete geographical coverage in southern Gansu, covering all the counties and districts governed by Gannan and Longnan (Figure 2). As Gannan and Longnan are located in mountainous areas, tap water samples were gathered along the winding roads in the mountains, which link residential areas. The total number of tap water and surface water samples were 1260 and 136, respectively. Information of all water samples is summed up in Table 1. In the division of four seasons, spring includes March, April and May, and summer includes June, July and August, and autumn includes September, October and November, and winter includes December, January (in the nest year) and February (in the nest year).

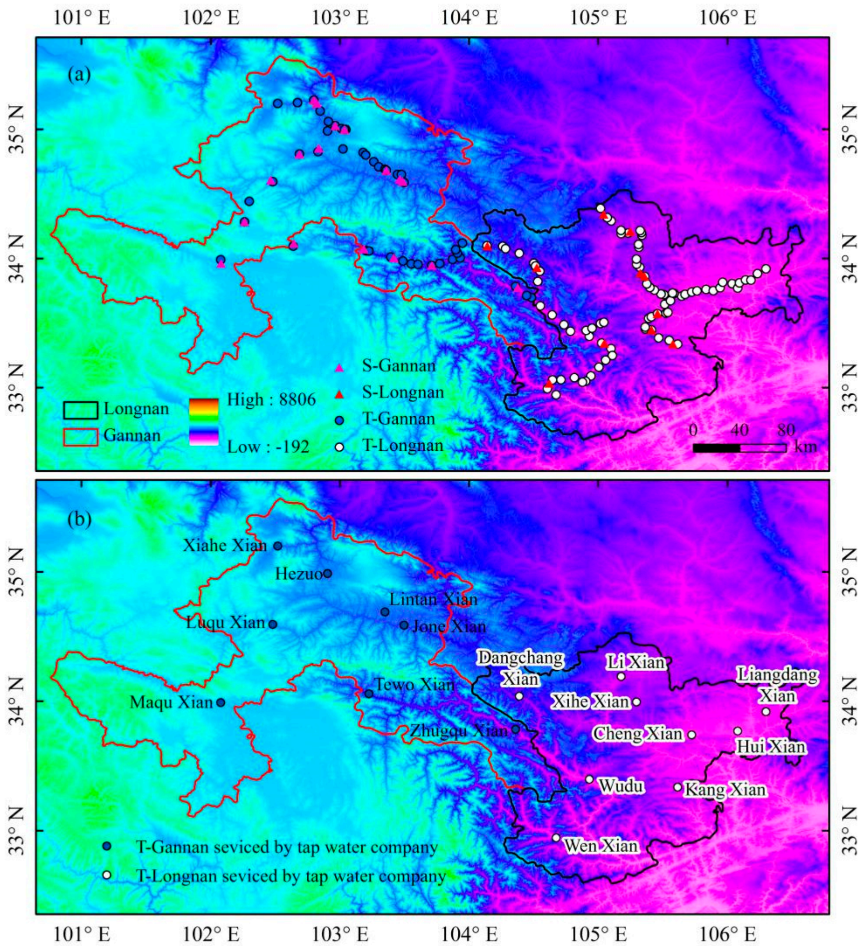

Figure 2. Spatial distribution of sampling sites in this study. (**a**) All of the tap water (T) and surface water (S) sampling sites in Gannan and Longnan. (**b**) Tap water sampling sites supplied centrally by tap water company in Gannan and Longnan (Table S1 in Supplementary Materials).

Table 1. Information of all collected water samples in Gannan and Longnan.

Water Type	Area	Number of Sampling Sites (N)	Sum of Sampling Sites	Sampling Frequency	Number of Samples (*n*)	Sum of Samples
Tap water	Gannan Longnan	43 80	123	monthly monthly	433 827	1260
Surface water	Gannan Longnan	17 11	28	seasonally seasonally	82 54	136

3.2. Experimental Analysis

δ^2H and $\delta^{18}O$ in water samples were analyzed by a liquid water isotope analyzer (DLT-100, developed by the Los Gatos Research company of the United States) [42] at the Northwest Normal University. In the test, three standard samples (standard No. 3: δ^2H: −96.4 ± 0.5‰, $\delta^{18}O$: −13.10 ± 0.15‰; standard No. 4: δ^2H: −51.0 ± 0.5‰, $\delta^{18}O$: −7.69 ± 0.15‰; standard No. 5: δ^2H: −9.5 ± 0.5‰, $\delta^{18}O$: −2.80 ± 0.15‰; provided by the LGR company) and six gathered water samples were considered as one group. Every sample was tested for six injections. Data of the first two needles were discarded because of the isotope memory effect, and values of the last four needles were calculated as final results [43,44]. The measurement uncertainties for $\delta^{18}O$ and δ^2H were no more than 0.2‰ and 0.6‰. Results tested were relative to the Vienna Standard Mean Ocean Water (VSMOW).

$$\delta_{\text{sample}} = \frac{\left(R_{\text{sample}} - R_{\text{standard}}\right)}{R_{\text{standard}}} \times 1000‰ \quad (1)$$

In Equation (1), Rsample presents the ratio of $^2H/^1H$ ($^{18}O/^{16}O$) in water samples. Rstandard shows the ratio of $^2H/^1H$ ($^{18}O/^{16}O$) in the VSMOW.

3.3. Other Data

Precipitation isotope data used in this paper were detected from a global data product, the Regionalized Cluster-based Water Isotope Prediction (RCWIP, Grabiszyńska, Poland) model version 1.00 [45–49], providing estimated δ^2H and $\delta^{18}O$ in precipitation (annual and monthly values). The reliability of this precipitation isotope database in China has been verified to be good [38].

3.4. Tap Water Isoscape Simulation and Error Test Methods

Based on the existing studies about the isoscapes in different water bodies (e.g., tap water and precipitation) [31,45,50–52], seven regression models combining spatial (including latitude (L, °), longitude (O, °), and elevation (E, m)) and meteorological factors (e.g., average temperature and precipitation) (Table 2) were selected and compared to develop the isoscape of tap water in southern Gansu. The Shuttle Radar Topography Mission 90M Resolution Raw Elevation Data (SRTMDEM 90M) were applied in isoscape models. Meteorological parameters, including average temperature (T; °C), precipitation (P; mm), wind speed (S; m/s), water pressure (V; kPa), and solar radiation (R; kJ/(m^2·day)), with 30 s spatial resolution involved in these models were selected from WorldClim-Global Climate Data (version 2) [53]. Simulation results for all of the seven regression models were evaluated based on adjusted determination coefficient ($r_{adj}{}^2$), mean absolute error (MAE), mean bias error (MBE), and root mean square error (RMSE) (Table 3). Models 6 and 7 were selected for the simulation of δ^2H and $\delta^{18}O$, respectively, as the optimal model. The simulated contour combined regression estimation and interpolated residuals with the Kriging method [36].

Table 2. Regression models for the estimation of tap water isoscape in Gannan and Longnan.

Code	Regression Model	Regression Method	Reference
1	$\delta = aL^2 + bL + cE + d$	Multiple regression	[36,50,52]
2	$\delta = aL + bO + cE + d$	Multiple regression	[34]
3	$\delta = aT + bP + c$	Multiple regression	[34]
4	$\delta = aT + bP + cR + dS + eV + f$	Multiple regression	[38]
5	L, O, E, L^2, O^2, E^2	Stepwise regression	[51]
6	$T, P, R, S, V, T^2, P^2, R^2, S^2, V^2$	Stepwise regression	[51,54]
7	$L, O, E, T, P, R, S, V, L^2, O^2, E^2, T^2, P^2, R^2, S^2, V^2$	Stepwise regression	[38]

Note: L, latitude (in degree); O, longitude (in degree); E, elevation (in m); T, temperature (in °C); P, precipitation (in mm); R, solar radiation (in kJ/(m^2·day)); S, wind speed (in m/s); V, water vapor pressure (in kPa).

Table 3. Equations of regression models for δ^2H and δ^{18}O in tap water in Gannan and Longnan.

Isotope	Code	Equations	r^2	r_{adj}^2	Sig.	N	MBE	MAE	RMSE
δ^2H (‰)	1	$\delta = 0.122L^2 - 0.012E - 182.913$	0.582	0.575	0.000	123	0.14	4.13	5.13
	2	$\delta = 5.61L + 5.317O - 0.004E - 803.075$	0.665	0.657	0.000	123	−0.66	3.67	4.65
	3	$\delta = 1.053T + 0.048P - 101.836$	0.436	0.426	0.000	123	−0.01	4.83	5.96
	4	$\delta = -4.505T - 0.058P + 0.00006449R - 10.554S + 99.162V - 64.208$	0.66	0.645	0.000	123	−0.08	3.67	4.63
	5	$\delta = 0.082L^2 + 0.025O^2 - 0.0000009622E^2 - 423.155$	0.672	0.664	0.000	123	4.20	4.84	6.19
	6	$\delta = -0.053P + 74.125S + 77.378V - 0.098T^2 - 16.107S^2 - 166.133$	0.709	0.696	0.000	123	0.02	3.26	4.28
	7	$\delta = -0.001R + 65.462V + 0.236L^2 - 0.096T^2 - 209.471$	0.730	0.721	0.000	123	10.53	10.53	11.31
δ^{18}O (‰)	1	$\delta = 0.021L^2 - 0.002E - 30.661$	0.541	0.533	0.000	123	−0.38	0.71	0.86
	2	$\delta = 0.889L + 1.057O - 0.00003615E - 150.125$	0.718	0.711	0.000	123	−0.01	0.45	0.57
	3	$\delta = 0.114T + 0.009P - 16.187$	0.408	0.399	0.000	123	−0.15	0.68	0.84
	4	$\delta = -0.545T - 0.006P + 0.00003996R - 0.41S + 13.941V - 18.462$	0.698	0.685	0.000	123	0.20	0.48	0.63
	5	$\delta = 0.013L^2 + 0.005O^2 - 80.602$	0.720	0.715	0.000	123	−1.47	1.48	1.58
	6	$\delta = -0.001R + 10.531V - 0.02T^2 + 0.000000003406R^2 + 61.186$	0.722	0.713	0.000	123	5.33	5.33	5.36
	7	$\delta = -0.000135R + 13.746S + 8.259V + 0.034L^2 - 3.086S^2 - 47.914$	0.793	0.784	0.000	123	0.27	0.41	0.56

Note: N, number of the tap water sampling sites; L, latitude (in degree); O, longitude (in degree); E, elevation (in m); T, temperature (in °C); P, precipitation (in mm); R, solar radiation (in kJ/(m^2·day)); S, wind speed (in m/s); V, water vapor pressure (in kPa); MBE, mean bias error; MAE, mean absolute error; RMSE, root mean square error.

4. Result

4.1. Basic Characteristics of Tap Water Isotopes

4.1.1. Local Tap Water Line

Figure 3 shows the local tap water line (LTWL), local surface water line (LSWL), and local meteoric water line (LMWL) in Gannan and Longnan. Global meteoric water line (GMWL), δ^2H = 8 δ^{18}O + 10 [55], is also presented in Figure 3. The LTWLs in Gannan and Longnan are δ^2H = (7.06 ± 0.17) δ^{18}O + (3.24 ± 1.75) ($r^2 = 0.81$, $p < 0.01$) and δ^2H = (5.66 ± 0.09) δ^{18}O + (−8.12 ± 0.82) ($r^2 = 0.82$, $p < 0.01$), respectively. Lower slopes can be seen in the LTWLs in Gannan and Longnan compared to the GMWL proposed by Craig [55] and Gourcy et al. (δ^2H = (8.14 ± 0.02) δ^{18}O + (10.9 ± 0.2), $r = 0.98$) [56] (in the Student's t-test, $p > 0.05$) [10]. The slopes of the LTWLs in Gannan and Longnan are also lower than the Chinese tap water line δ^2H = (7.57 ± 0.04) δ^{18}O + (5.07 ± 0.38) ($r^2 = 0.93$, $p < 0.01$) (in the Student's t-test, $p > 0.05$) [10], newly calculated combining two exciting data sets of Chinese tap water isotopes (base on monthly tap water isotope values) [34,38]. This may be as a result of differences in climate and evaporation ratios in water source areas [57]. The slopes of LTWLs, LSWLs, and LMWLs are all higher in Gannan than those in Longnan.

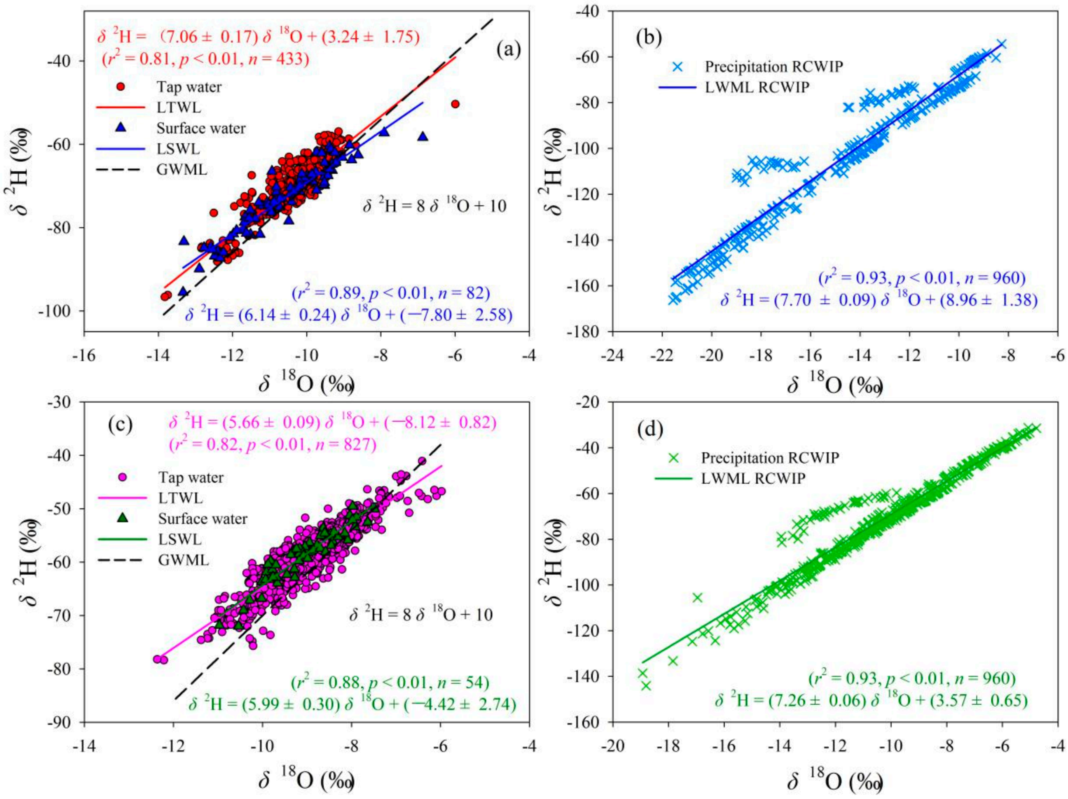

Figure 3. Relationships between δ^2H and δ^{18}O in tap water, surface water, and precipitation in Gannan and Longnan; (**a**,**b**) Gannan, (**c**,**d**) Longnan. (GMWL: Global meteoric water line; LMWL: Local meteoric water line; LTWL: Local tap water line; LSWL: Local surface water line; *n*: Number of water samples or grid sites).

4.1.2. Spatial Pattern

The simulated tap water isoscape in Gannan and Longnan is exhibited in Figure 4 and Figure S1 (in Supplementary Materials). From southwest to northeast, the annual mean δ^2H and δ^{18}O show an increasing trend on the whole. In southwest Gannan, isotopes are the lowest within Gannan, with δ^2H values lower than −85.0‰ and δ^{18}O lower than −11.0‰. In the north and east parts of Gannan, annual mean δ^2H and δ^{18}O in tap water are the highest within Gannan, with some δ^2H values higher than −75.0‰ and δ^{18}O higher than −10.0‰. In most parts of Gannan, the annual mean values of δ^2H range from −85.0 to −65.0‰ and those of δ^{18}O are lower than −11.0‰. Isotopes in Longnan are higher than those in Gannan in general. In most parts of Longnan, the annual mean values of δ^2H are higher than −65.0‰ and those of δ^{18}O are higher than −10.0‰. The annual mean values of δ^2H in tap water in the east part of Longnan are the highest (δ^2H higher than −55.0‰), and those of δ^{18}O in southeast Longnan are the highest (δ^{18}O higher than −8.0‰). The simulated residuals for δ^2H and δ^{18}O are in Figure 4c,d. In most parts of Gannan and Longnan, residuals for δ^2H range between −2.0 and 2.0‰, and those for δ^{18}O are from −0.6 to 0.6‰. A jackknife procedure was applied to report the isoscape uncertainties (Figure 5). Each sampling site supplied centrally by tap water company (Figure 2, Table S1 in Supplementary Materials) in Gannan and Longnan was removed separately to simulate the isotope landscape. Correction between estimated and observation annual mean values of δ^2H and δ^{18}O is showed in Figure 5. The equations of δ^2H and δ^{18}O are close to y = x. The values of r^2 for the equations of δ^2H and δ^{18}O are 0.85 and 0.93, respectively. The simulated water isotope landscape map has a good accuracy.

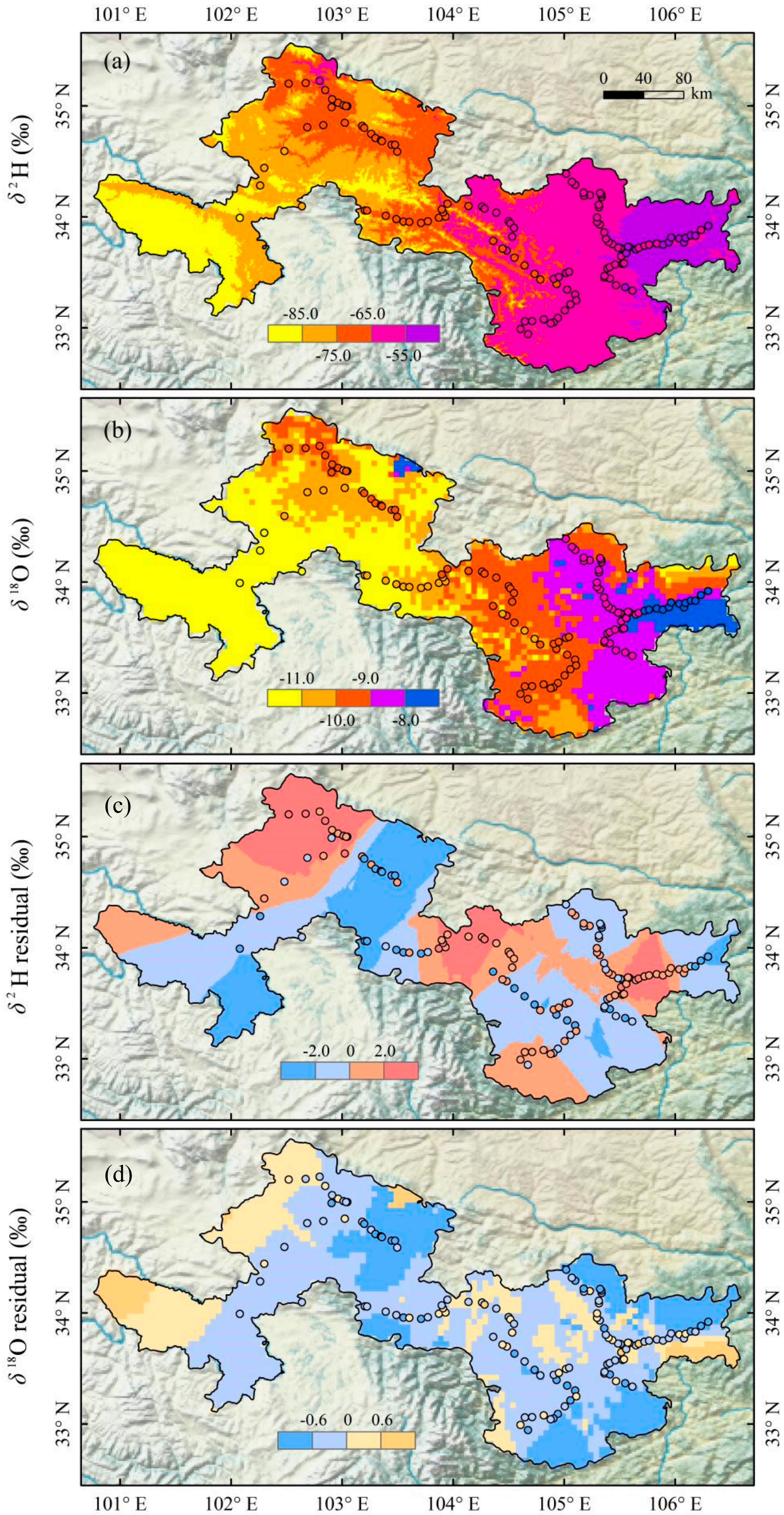

Figure 4. Spatial variations of annual mean values of δ^2H ((**a**), ‰) and δ^{18}O ((**b**), ‰) and residuals for δ^2H ((**c**), ‰) and δ^{18}O ((**d**), ‰) in tap water in Gannan and Longnan. Residuals equal to the observation values minus the estimated values.

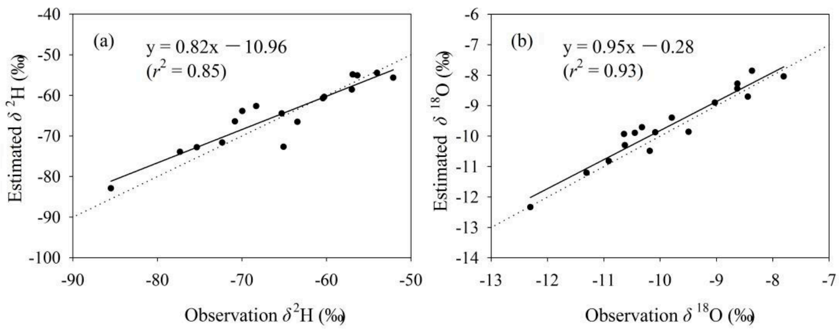

Figure 5. Correction between estimated and observation annual mean values of δ^2H ((**a**), ‰) and δ^{18}O ((**b**), ‰) in tap water at the sampling sites supplied centrally by tap water company (Table S1 in Supplementary Materials) in Gannan and Longnan. The dotted line is y = x.

4.1.3. Temporal Variation

Differences of isotope between two adjacent seasons ($\Delta\delta^2$H and $\Delta\delta^{18}$O, ‰) at every sampling site were calculated (Figure 6). On the whole, $\Delta\delta^2$H and $\Delta\delta^{18}$O between two adjacent seasons in Gannan and Longnan are small. The values of $\Delta\delta^2$H between two adjacent seasons mainly range from −3.0 to 2.0‰ (red and purple sampling sites in Figure 6a,c,e,g). The values of $\Delta\delta^{18}$O between spring and winter mainly vary from 0 to 0.5‰ (purple and dark purple sampling sites in Figure 6h), and those of $\Delta\delta^{18}$O between other two adjacent seasons are mainly from −0.5 to 0.2‰ (red and purple sampling sites in Figure 6b,d,f). Table 4 shows the seasonal and annual mean δ^2H and δ^{18}O in Gannan and Longnan. The highest seasonal mean δ^2H in Gannan and Longnan both appear in summer. The annual mean δ^2H and δ^{18}O in Gannan are both lower than those in Longnan.

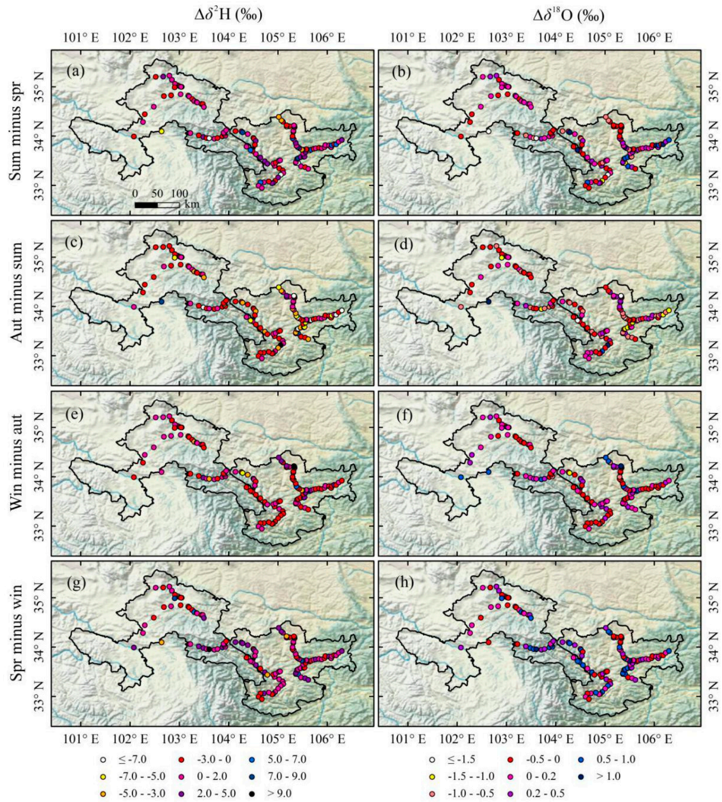

Figure 6. Differences for δ^2H and δ^{18}O (that is, $\Delta\delta^2$H and $\Delta\delta^{18}$O, ‰) in tap water in two adjacent seasons at each sampling site in Gannan and Longnan; (**a**,**b**) summer minus spring, (**c**,**d**) autumn minus summer, (**e**,**f**) winter minus autumn, (**g**,**h**) spring minus winter.

Table 4. Seasonal and annual mean δ^2H and δ^{18}O in tap water at all sampling sites in Gannan and Longnan.

Isotope	Area	Spring	Summer	Autumn	Winter	Annual
δ^2H (‰)	Gannan	−70.3	−70.0	−71.0	−71.2	−70.6
	Longnan	−58.4	−57.4	−59.2	−59.5	−58.6
δ^{18}O (‰)	Gannan	−10.3	−10.4	−10.6	−10.6	−10.5
	Longnan	−8.8	−8.8	−9.0	−9.1	−8.9

4.2. Comparison of Isotopes in Tap Water under Different Water Supply Modes with Those in Precipitation and Surface Water

4.2.1. Under the Mode of Central Water Supply by Local Tap Water Company

To detect the connection of tap water isotopes under different water supply modes with other water bodies, tap water samples under the mode of centralized water supply by local tap water companies in Gannan and Longnan (Figure 2b, Table S1 in Supplementary Materials) were selected and analyzed. On the whole, the correlation of isotopes between tap water supplied centrally by local water companies and precipitation is weak in Gannan and Longnan (Table 5). The correlation coefficients at most sampling sites are less than 0.5. In Figure 7, the correlation coefficients in the fitting equations for δ^2H and δ^{18}O between tap water and surface water in Gannan (r < 0.5) are smaller than those in Longnan (r > 0.5). Relatively speaking, weak connection of isotopes can be seen between tap water and surface water in Gannan, while better connection presents in Longnan.

Table 5. Correlation coefficients (r) of monthly δ^2H and δ^{18}O between tap water and precipitation under the mode of central water supply by local tap water companies in Gannan and Longnan.

Area	Sampling Sites	r of δ^2H	p < 0.05 (Yes/No)	r of δ^{18}O	p < 0.05 (Yes/No)
Gannan	Hezuo	0.31	N	0.49	N
	Xiahe Xian	0.45	N	0.59	N
	Lintan Xian	0.85	Y	0.92	Y
	Jone Xian	0.70	Y	0.75	Y
	Luqu Xian	0.19	N	−0.24	N
	Maqu Xian	0.59	N	0.36	N
	Tewo Xian	0.49	N	0.16	N
	Zhugqu Xian	−0.16	N	0.25	N
Longnan	Wudu	0.12	N	0.53	N
	Dangchang Xian	0.55	N	0.47	N
	Wen Xian	−0.73	Y	−0.47	N
	Kang Xian	0.24	N	0.51	N
	Cheng Xian	0.59	N	0.54	N
	Hui Xian	0.26	N	0.12	N
	Liangdang Xian	0.46	N	0.54	N
	Xihe Xian	0.35	N	0.32	N
	Li Xian	0.48	N	0.31	N

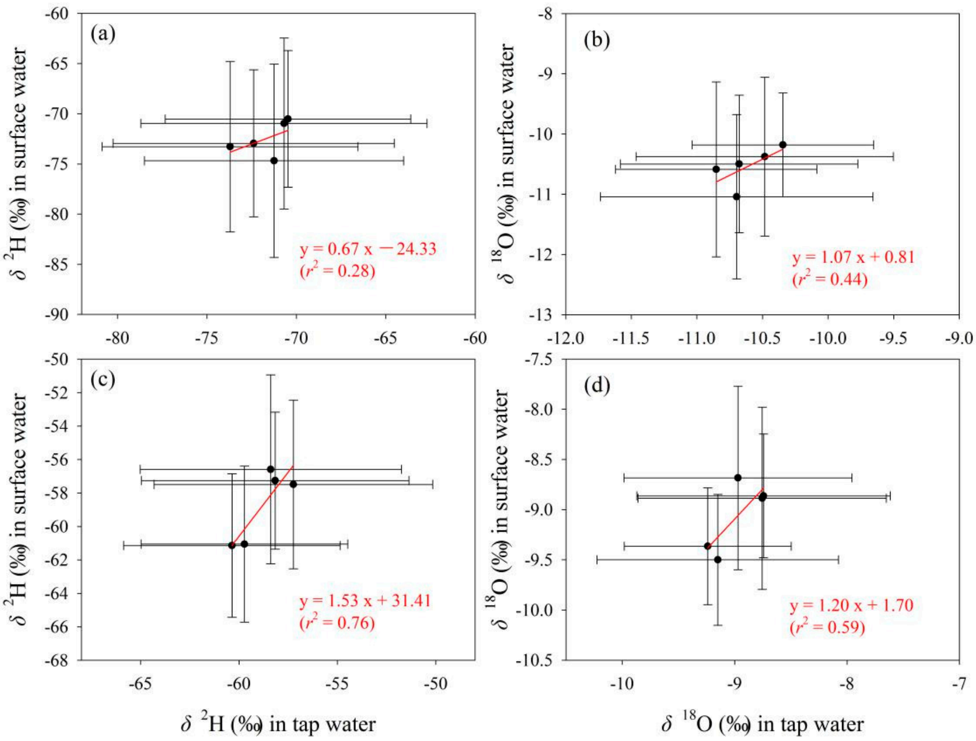

Figure 7. Relationship of δ^2H and δ^{18}O (‰) in tap water under the mode of centralized water supply by local tap water companies with those in surface water in Gannan (**a**,**b**) and Longnan (**c**,**d**). Solid circles and error bars show the arithmetic average and standard deviation, respectively.

4.2.2. Under Mixed Tap Water Supply Modes

The relationship between isotopes in tap water under mixed water supply modes (based on all tap water samples) and those in other two water bodies in Longnan and Gannan was analyzed in detail in terms of temporal variation, numerical difference, and correlation. In general, the temporal features of isotopes between in tap water under mixed water supply modes and precipitation show great differences (Figure 8). The monthly δ^2H in Gannan and Longnan change little throughout the year, and so are the δ^{18}O values. Isotopes in precipitation in Gannan are higher in summer, with lower values in winter. In Longnan, the seasonal mean δ^2H and δ^{18}O in precipitation are the highest in spring (δ^2H: −53.7‰, δ^{18}O: −7.8‰) and the lowest (δ^2H: −82.0‰, δ^{18}O: −11.6‰) in winter. The isotopic seasonal differences of surface water are small, so are tap water (Figure 9). The lowest seasonal values δ^2H (−74.7‰) and δ^{18}O (−11.0‰) in surface water in Gannan present in autumn. The highest seasonal values δ^2H (−57.1‰) and δ^{18}O (−8.8‰) in surface water in Longnan appear in spring.

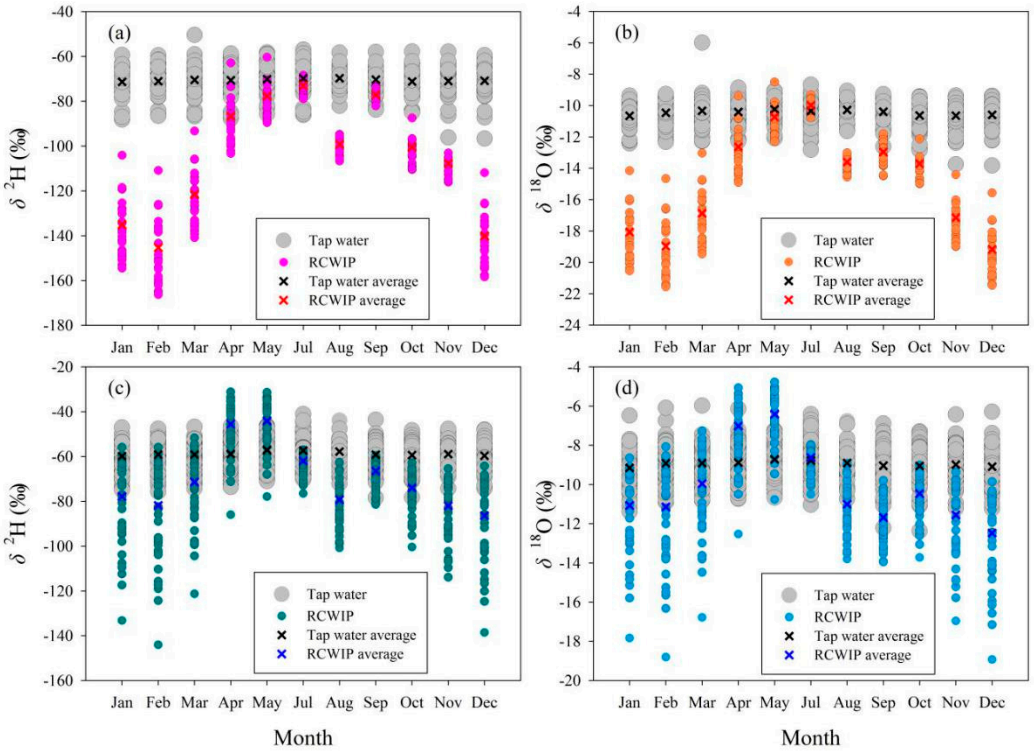

Figure 8. Comparison of monthly δ^2H and δ^{18}O (‰) between tap water and precipitation in Gannan (**a**,**b**) and Longnan (**c**,**d**).

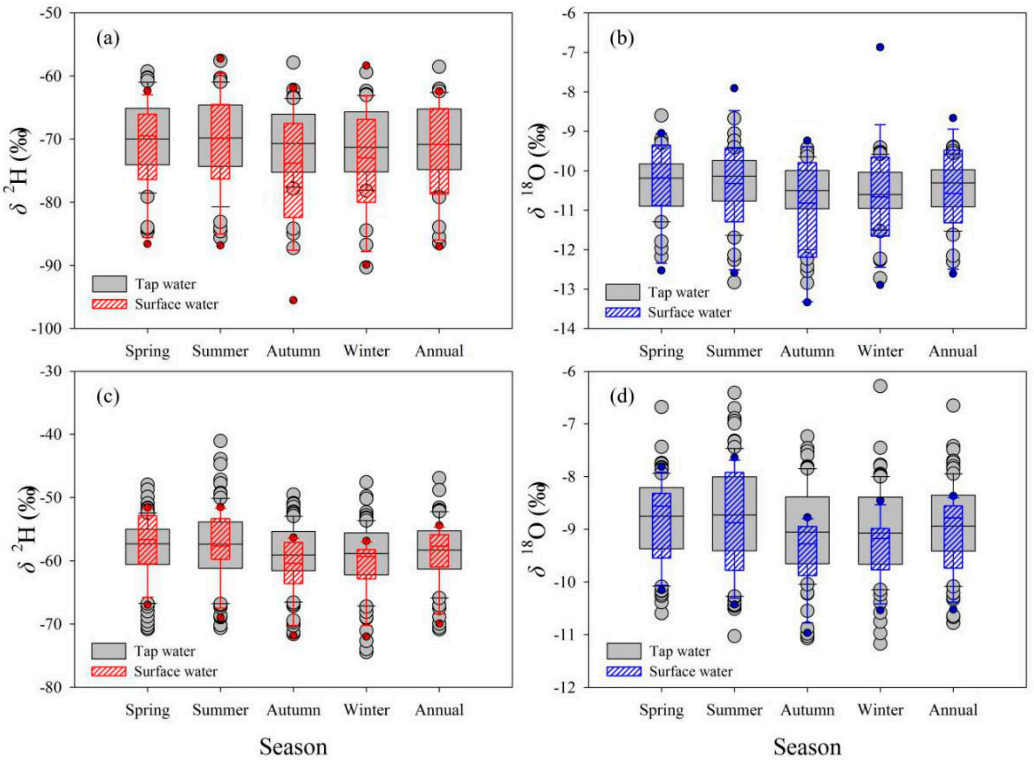

Figure 9. Comparison of seasonal and annual δ^2H and δ^{18}O (‰) between tap water and surface water in Gannan (**a**,**b**) and Longnan (**c**,**d**). The top and bottom of the box exhibit the 75th and 25th percentiles, the line in the box signs the 50th percentile (median), whiskers mark the 10th and 90th percentiles; points below and above the whiskers indicate lower than the 10th and higher than 90th percentiles, respectively.

Numerical differences of tap water isotopes with precipitation are much larger than those with surface water (Figure 10). Differences of monthly mean δ^2H in tap water with that in precipitation in Gannan and Longnan mainly range from 0 to 30.0‰ (Figure 10a), and those for δ^{18}O mainly range from −2.0 to 4.0‰ (Figure 10b). The differences of monthly mean δ^2H and δ^{18}O between tap water and precipitation in Gannan are larger than those in Longnan (Figure 10a,b). The differences of seasonal mean δ^2H in tap water with surface water in Gannan and Longnan mainly range from −1.0 to 3.0‰ (Figure 10c), and those for δ^{18}O mainly range from −0.1 to 0.4‰ (Figure 10d). Differences of seasonal mean δ^2H between surface water and tap water in Gannan are larger than those in Longnan (Figure 10c,d).

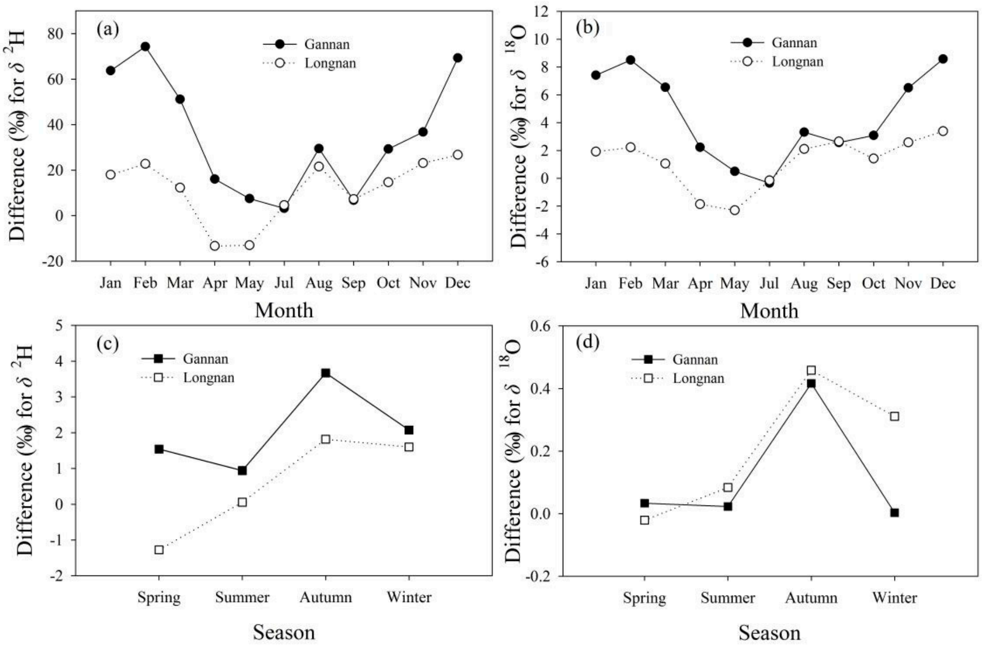

Figure 10. Differences (‰) of δ^2H and δ^{18}O in tap water with precipitation and surface water in Gannan and Longnan. (**a**,**b**) tap water minus precipitation, (**c**,**d**) tap water minus surface water.

The relationships of δ^2H and δ^{18}O in tap water with those in the other two water bodies are presented in Figures 11 and 12, respectively. Overall, tap water isotopes show better correlation with surface water than precipitation. As δ^2H and δ^{18}O values in surface water increase, those in tap water show an upward trend (Figure 12). In contrast, with the increasing of δ^2H and δ^{18}O in precipitation, those in tap water do not show a uniform changing trend (Figure 11). For tap water and precipitation, the correlation coefficients in the fitting equations for δ^2H and δ^{18}O are all less than 0.5 in Gannan and Longnan (Figure 11). To tap water and surface water, those for δ^2H and δ^{18}O are all larger than 0.7 (Figure 12).

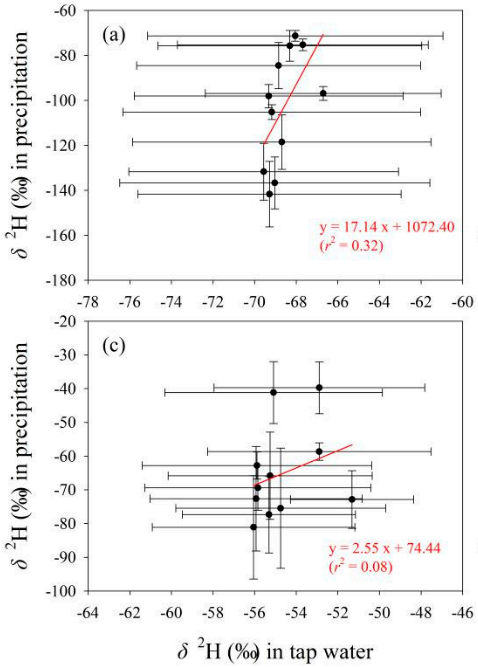

Figure 11. Relationship of δ^2H and $\delta^{18}O$ (‰) between tap water and precipitation in Gannan (**a**,**b**) and Longnan (**c**,**d**). Solid circles and error bars show the arithmetic average and standard deviation, respectively.

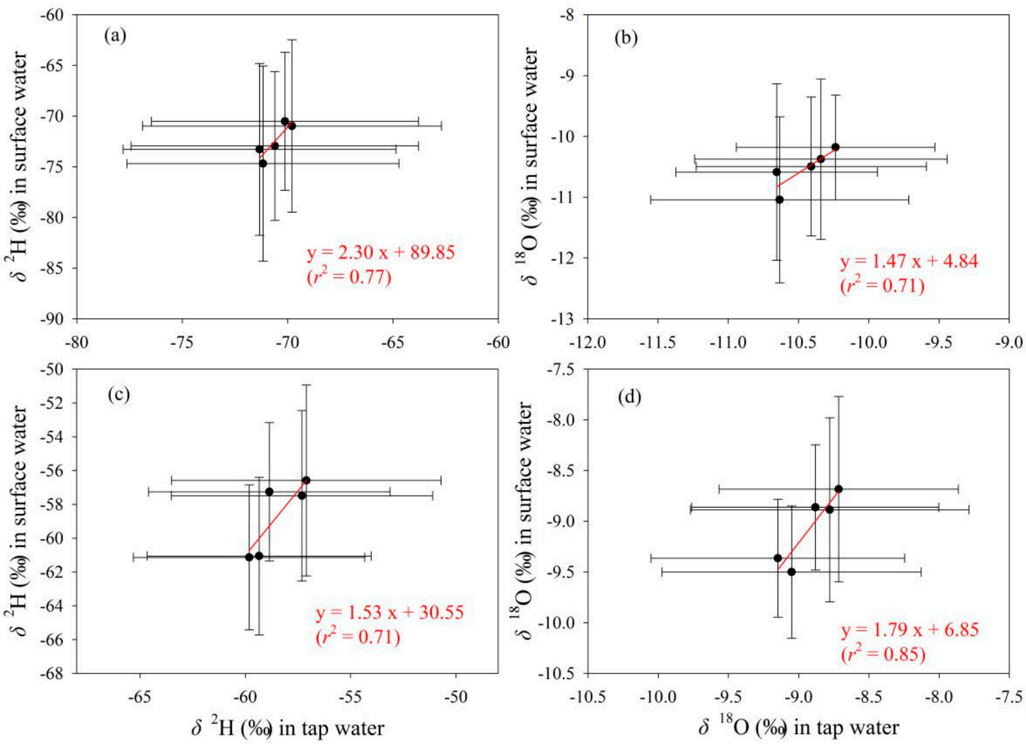

Figure 12. Relationship of δ^2H and $\delta^{18}O$ (‰) between tap water and surface water in five seasonal sampling times in Gannan (**a**,**b**) and Longnan (**c**,**d**). Solid circles and error bars show the arithmetic average and standard deviation, respectively.

5. Discussion on Water Source Information of Tap Water Isotopes

Under the mode of central water supply by local tap water companies, for tap water isotopes, weak connection can be seen in Gannan with isotopes in precipitation and surface water, while tap water isotopes in Longnan present better correlation with surface water isotopes. According to water supply information from tap water companies and our field investigation data about water source, groundwater and surface water are the main tap water sources in Gannan and Longnan, respectively, under the this mode of water supply. Correlation of tap water isotopes with isotopic composition of main water source is high, while that with isotopic composition of non-water source is low.

Under mixed tap water supply modes, in Gannan and Longnan, tap water isotopes both show better correlation with isotopic composition of surface water, including seasonal variations, numerical differences, and correlation. On the basis of our field investigation data, tap water sampling sites with surface water as water source account for larger proportion, both in Gannan and Longnan, compared with other water sources (precipitation and groundwater). It can be found that isotopes in tap water can well indicate the main water source, in the case of multiple water sources.

6. Conclusions

The isotopic composition in tap water shows great significance for the understanding of local natural and humanistic environment background, water supply management, and regional water resources. In this study, δ^2H and δ^{18}O in 1260 tap water and 136 surface water samples were analyzed to exhibit the spatiotemporal characteristics of tap water isotopes and their water source signals under different water supply modes. Main results are: The LTWLs in Gannan and Longnan are $\delta^2H = (7.06 \pm 0.17)\ \delta^{18}O + (3.24 \pm 1.75)$ ($r^2 = 0.81$, $p < 0.01$) and $\delta^2H = (5.66 \pm 0.09)\ \delta^{18}O + (-8.12 \pm 0.82)$ ($r^2 = 0.82$, $p < 0.01$), respectively. Isotopes in tap water show an increasing trend from southwest to northeast, and their seasonal differences are small. Correlation of tap water isotopes with isotopic composition of main water source is high, while that with isotopic composition of non-water source is low. Under the central water supply mode by local tap water companies, tap water isotopes in Gannan where groundwater is the direct water source show weak connection with isotopes in surface water and precipitation, and for tap water isotopes in Longnan where surface water is the main water source, good connection present with surface water isotopes. Under mixed water supply modes, tap water isotopes indicate that surface water is the main source of tap water in Gannan and Longnan. Isotopic composition of tap water can well indicate the main water source, in the case of multiple water sources.

Supplementary Materials: The following are available online at http://www.mdpi.com/2073-4441/11/12/2578/s1: Table S1. Information of tap water sampling sites serviced by tap water companies among all the tap water sampling sites in Gannan and Longnan; Figure S1. Spatial variations of annual mean values of *d*-excess (‰) in tap water in Gannan and Longnan. The map of *d*-excess was calculated according to d-excess = $\delta^2H - 8\ \delta^{18}O$, based on the maps of δ^2H and δ^{18}O.

Author Contributions: Sample collection, H.M. and C.C.; experimental analysis and writing—original draft preparation, M.D.; writing—review and editing, S.W. and R.G.; funding acquisition, M.Z.

Funding: This research was supported by the National Natural Science Foundation of China (No. 41701028), and the Scientific Research Program of Higher Education Institutions of Gansu Province (No. 2018C-02).

Acknowledgments: The authors are very thankful for the team partners' help during the processes of sample collection and experiment analysis.

Conflicts of Interest: The authors declare no conflict of interest.

References

1. Killingley, J.S.; Newman, W.A. ^{18}O fractionation in barnacle calcite: A barnacle paleotemperature equation. *J. Mar. Res.* **1982**, *40*, 893–902.
2. Gat, J.R. Oxygen and hydrogen isotopes in the hydrologic cycle. *Annu. Rev. Earth Planet. Sci.* **1996**, *24*, 225–262. [CrossRef]

3. Roden, J.S.; Lin, G.G.; Ehleringer, J.R. A mechanistic model for interpretation of hydrogen and oxygen isotope ratios in tree-ring cellulose. *Geochim. Cosmochim. Acta* **2000**, *64*, 21–35. [CrossRef]
4. Harvey, F.E.; Sibray, S.S. Delineating ground water recharge from leaking irrigation canals using water chemistry and isotopes. *Ground Water* **2001**, *39*, 408–421. [CrossRef]
5. Yepez, E.A.; Williams, D.G.; Scott, R.L.; Lin, G. Partitioning overstory and understory evapotranspiration in a semiarid savanna woodland from the isotopic composition of water vapor. *Agric. For. Meteorol.* **2003**, *119*, 53–68. [CrossRef]
6. Burnett, A.W.; Mullins, H.T.; Patterson, W.P. Relationship between atmospheric circulation and winter precipitation delta O-18 in central New York State. *Geophys. Res. Lett.* **2004**, *31*, L22209. [CrossRef]
7. Williams, D.G.; Cable, W.; Hultine, K.; Hoedjes, J.C.B.; Yepez, E.A.; Simonneaux, V.; Er-Raki, S.; Boulet, G.; de Bruin, H.A.R.; Chehbouni, A. Evapotranspiration components determined by stable isotope, sap flow and eddy covariance techniques. *Agric. For. Meteorol.* **2004**, *125*, 241–258. [CrossRef]
8. West, J.B.; Bowen, G.J.; Cerling, T.E.; Ehleringer, J.R. Stable isotopes as one of nature's ecological recorders. *Trends Ecol. Evol.* **2006**, *21*, 408–414. [CrossRef]
9. Ehleringer, J.R.; Bowen, G.J.; Chesson, L.A.; West, A.G.; Podlesak, D.W.; Cerling, T.E. Hydrogen and oxygen isotope ratios in human hair are related to geography. *Proc. Natl. Acad. Sci. USA* **2008**, *105*, 2788–2793. [CrossRef]
10. Boschetti, T.; Cifuentes, J.; Iacumin, P.; Selmo, E. Local Meteoric Water Line of Northern Chile (18 S—30 S): An application of error-in-variables regression to the oxygen and hydrogen stable isotope ratio of precipitation. *Water* **2019**, *11*, 791. [CrossRef]
11. Gat, J.R.; Bowser, C.J.; Kendall, C. The contribution of evaporation from the Great Lakes to the continental atmosphere: Estimate based on stable isotope data. *Res. Lett.* **1994**, *21*, 557–560. [CrossRef]
12. Hobson, K.A.; Atwell, L.; Wassenaar, L.I. Influence of drinking water and diet on the stable-hydrogen isotope ratios of animal tissues. *Proc. Natl. Acad. Sci. USA* **1999**, *96*, 8003–8006. [CrossRef]
13. Gibson, J.J.; Edwards, T.W.D. Regional water balance trends and evaporation-transpiration partitioning from a stable isotope survey of lakes in northern Canada. *Glob. Biogeochem. Cycles* **2002**, *16*, 1026. [CrossRef]
14. Bowen, G.J.; Wassenaar, L.I.; Hobson, K.A. Global application of stable hydrogen and oxygen isotopes to wildlife forensics. *Oecologia* **2005**, *143*, 337–348. [CrossRef]
15. Kelly, S.; Heaton, K.; Hoogewerff, J. Tracing the geographical origin of food: The application of multi-element and multi-isotope analysis. *Trends Food Sci. Technol.* **2005**, *16*, 555–567. [CrossRef]
16. McGuire, K.J.; McDonnell, J.J.; Weiler, M.; Kendall, C.; McGlynn, B.L.; Welker, J.M.; Seibert, J. The role of topography on catchment–scale water residence time. *Water Resour. Res.* **2005**, *41*, W05002. [CrossRef]
17. West, A.G.; Hultine, K.R.; Burtch, K.G.; Ehleringer, J.R. Seasonal variations in moisture use in a pinon-juniper woodland. *Oecologia* **2007**, *153*, 787–798. [CrossRef]
18. Worden, J.; Noone, D.; Bowman, K.; Beer, R.; Eldering, A.; Fisher, B.; Gunson, M.; Goldman, A.; Herman, R.; Kulawik, S.S.; et al. Importance of rain evaporation and continental convection in the tropical water cycle. *Nature* **2007**, *445*, 528–532. [CrossRef]
19. Hawkins, H.; Hettasch, H.; West, A.G.; Cramer, M.D. Hydraulic redistribution by Protea "Sylvia" (Proteaceae) facilitates soil water replenishment and water acquisition by an understorey grass and shrub. *Funct. Plant Biol.* **2009**, *36*, 752–760. [CrossRef]
20. Brooks, J.R.; Barnard, H.R.; Coulombe, R.; McDonnell, J.J. Ecohydrologic separation of water between trees and streams in a Mediterranean climate. *Nat. Geosci.* **2010**, *3*, 100–104. [CrossRef]
21. Bowen, G.J.; Kennedy, C.D.; Henne, P.D.; Zhang, T. Footprint of recycled water subsidies downwind of Lake Michigan. *Ecosphere* **2012**, *3*, 1–16. [CrossRef]
22. Brienen, R.J.W.; Helle, G.; Pons, T.L.; Guyot, J.L.; Gloor, M. Oxygen isotopes in tree rings are a good proxy for Amazon precipitation and El Nino-Southern Oscillation variability. *Proc. Natl. Acad. Sci. USA* **2012**, *109*, 16957–16962. [CrossRef]
23. Bowen, G.J.; Winter, D.A.; Spero, H.J.; Zierenberg, R.A.; Reeder, M.D.; Cerling, T.E.; Ehleringer, J.R. Stable hydrogen and oxygen isotope ratios of bottled waters of the world. *Rapid Commun. Mass Spectrom.* **2005**, *19*, 3442–3450. [CrossRef] [PubMed]
24. Brenčič, M.; Vreča, P. Identification of sources and production processes of bottled waters by stable hydrogen and oxygen isotope ratios. *Rapid Commun. Mass Spectrom.* **2006**, *20*, 3205–3212. [CrossRef] [PubMed]
25. Bong, Y.S.; Ryu, J.S.; Lee, K.S. Characterizing the origins of bottled water on the South Korean market using chemical and isotopic compositions. *Anal. Chim. Acta* **2009**, *631*, 189–195. [CrossRef]

26. Chesson, L.A.; Valenzuela, L.O.; O'Grady, S.P.; Cerling, T.E.; Ehleringer, J.R. Hydrogen and oxygen stable isotope ratios of milk in the United States. *J. Agric. Food Chem.* **2010**, *58*, 2358–2363. [CrossRef]
27. Chesson, L.A.; Valenzuela, L.O.; O'Grady, S.P.; Cerling, T.E.; Ehleringer, J.R. Links between purchase location and stable isotope ratios of bottled water, soda, and beer in the United States. *J. Agric. Food Chem.* **2010**, *58*, 7311–7316. [CrossRef]
28. Dotsika, E.; Poutoukis, D.; Raco, B.; Psomiadis, D. Stable isotope composition of Hellenic bottled waters. *J. Geochem. Explor.* **2010**, *107*, 299–304.
29. Kim, G.E.; Shin, W.J.; Ryu, J.S.; Choi, M.S.; Lee, K.S. Identification of the origin and water type of various Korean bottled waters using strontium isotopes. *J. Geochem. Explor.* **2013**, *132*, 1–5. [CrossRef]
30. Li, S.; Levin, N.E.; Chesson, L.A. Continental scale variation in ^{17}O-excess of meteoric waters in the United States. *Geochim. Cosmochim. Acta* **2015**, *164*, 110–126. [CrossRef]
31. West, A.G.; February, E.C.; Bowen, G.J. Spatial analysis of hydrogen and oxygen stable isotopes ("isoscapes") inground water and tap water across South Africa. *J. Geochem. Explor.* **2014**, *145*, 213–222. [CrossRef]
32. Jameel, Y.; Brewer, S.; Good, S.P.; Tipple, B.J.; Ehleringer, J.R.; Bowen, G.J. Tap water isotope ratios reflect urban water system structure and dynamics across a semi-arid metropolitan area. *Water Resour. Res.* **2016**, *52*, 1–20. [CrossRef]
33. Tipple, B.J.; Jameel, Y.; Chau, T.H.; Mancuso, C.J.; Bowen, G.J.; Dufour, A.; Chesson, L.A.; Ehleringer, J.R. Stable hydrogen and oxygen isotopes of tap water reveal structure of the San Francisco Bay Area's water system and adjustments during a major drought. *Water Res.* **2017**, *119*, 212–224. [CrossRef] [PubMed]
34. Zhao, S.; Hu, H.; Tian, F.; Tie, Q.; Wang, L.; Liu, Y.; Shi, C. Divergence of stable isotopes in tap water across China. *Sci. Rep.* **2017**, *7*, 43653. [CrossRef] [PubMed]
35. Good, S.P.; Kennedy, C.D.; Stalker, J.C.; Chesson, L.A.; Valenzuela, L.O.; Beasley, M.M.; Ehleringer, J.R.; Bowen, G.J. Patterns of local and nonlocal water resource use across the western US determined via stable isotope intercomparisons. *Water Resour. Res.* **2014**, *50*, 8034–8049. [CrossRef]
36. Bowen, G.J.; Ehleringer, J.R.; Chesson, L.A.; Stange, E.; Cerling, T.E. Stable isotope ratios of tap water in the contiguous United States. *Water Resour. Res.* **2007**, *43*, 399–407. [CrossRef]
37. Landwehr, J.M.; Coplen, T.B.; Stewart, D.W. Spatial, seasonal, and source variability in the stable oxygen and hydrogen isotopic composition of tap waters throughout the USA. *Hydrol. Process.* **2014**, *28*, 5382–5422. [CrossRef]
38. Wang, S.; Zhang, M.; Bowen, G.J.; Liu, X.; Du, M.; Chen, F.; Qiu, X.; Wang, L.; Che, Y.; Zhao, G. Water source signatures in the spatial and seasonal isotope variation of Chinese tap waters. *Water Resour. Res.* **2018**. [CrossRef]
39. Jiang, Y. China's water security: Current status, emerging challenges and future prospects. *Environ. Sci. Policy* **2015**, *54*, 106–125. [CrossRef]
40. Du, M.; Zhang, M.; Wang, S.; Chen, F.; Zhao, P.; Zhou, S.; Zhang, Y. Stable Isotope Ratios in Tap Water of a Riverside City in a Semi-Arid Climate: An Application to Water Source Determination. *Water* **2019**, *11*, 1441. [CrossRef]
41. Clark, I.; Fritz, P. *Environmental Isotopes in Hydrogeology*; CRC Press: New York, NY, USA, 1997; p. 328.
42. Newman, B.; Tanweer, A.; Kurttas, T. *IAEA Standard Operating Procedure for the Liquid-Water Stable Isotope Analyser, Laser Procedure*; IAEA Water Resources Programme; IAEA: Vienna, Austria, 2009; p. 27.
43. Lis, G.; Wassenaar, L.I.; Hendry, M.J. High-precision laser spectroscopy D/H and ^{18}O/^{16}O measurements of microliter natural water samples. *Anal. Chem.* **2008**, *80*, 287–293. [CrossRef] [PubMed]
44. Lyon, S.W.; Desilets, S.L.E.; Troch, P.A. A tale of two isotopes: Differences in hydrograph separation for a runoff event when using δD versus δ^{18}O. *Hydrol. Process.* **2009**, *23*, 2095–2101. [CrossRef]
45. Terzer, S.; Wassenaar, L.I.; Araguás-Araguás, L.J.; Aggarwal, P.K. Global isoscapes for δ^{18}O and δ^{2}H in precipitation: Improved prediction using regionalized climatic regression models. *Hydrol. Earth Syst. Sci.* **2013**, *17*, 4713–4728. [CrossRef]
46. IAEA (International Atomic Energy Agency). *Regionalized Cluster-Based Water Isotope Prediction (RCWIP)*. 2018. Available online: http://www-naweb.iaea.org/napc/ih/IHS_resources_rcwip.html (accessed on 25 April 2019).
47. IAEA/WMO (International Atomic Energy Agency/World Meteorological Organization). *Water Isotope System for Data Analysis, Visualization and Electronic Retrieval (WISER)*. 2017. Available online: https://nucleus.iaea.org/wiser (accessed on 12 March 2019).

48. Christner, E.; Kohler, M.; Schneider, M. The influence of snow sublimation and meltwater evaporation on δD of water vapor in the atmospheric boundary layer of central Europe. *Atmos. Chem. Phys.* **2017**, *17*, 1207–1225. [CrossRef]
49. Seltzer, A.M.; Buizert, C.; Baggenstos, D.; Brook, E.J.; Ahn, J.; Yang, J.-W.; Severinghaus, J.P. Does δ^{18}O of O_2 record meridional shifts in tropical rainfall? *Clim. Past* **2017**, *13*, 1323–1338. [CrossRef]
50. Bowen, G.J.; Revenaugh, J. Interpolating the isotopic composition of modern meteoric precipitation. *Water Resour. Res.* **2003**, 39. [CrossRef]
51. Lykoudis, S.P.; Argiriou, A.A. Gridded data set of the stable isotopic composition of precipitation over the eastern and central Mediterranean. *J. Geophys. Res.* **2007**, *112*, D18107. [CrossRef]
52. Liu, Z.; Tian, L.; Chai, X.; Yao, T. A model-based determination of spatial variation of precipitation δ^{18}O over China. *Chem. Geol.* **2008**, *249*, 203–212. [CrossRef]
53. Fick, S.E.; Hijmans, R.J. WorldClim 2: New 1-km spatial resolution climate surfaces for global land areas. *Int. J. Climatol.* **2017**, *37*, 4302–4315. [CrossRef]
54. Liu, J.; Song, X.; Yuan, G.; Sun, X.; Yang, L. Stable isotopic compositions of precipitation in China. *Tellus B Chem. Phys. Meteorol.* **2014**, *66*, 22567. [CrossRef]
55. Craig, H. Isotopic variations in meteoric waters. *Science* **1961**, *133*, 1702–1703. [CrossRef] [PubMed]
56. Gourcy, L.L.; Groening, M.; Aggarwal, P.K. Stable oxygen and hydrogen isotopes in precipitation. In *Isotopes in the Water Cycle: Past, Present and Future of Developing Science*; Aggarwal, P.K., Gat, J.R., Froehlich, K.F.O., Eds.; Springer: Dordrecht, The Netherlands, 2005; pp. 39–51. [CrossRef]
57. Salati, E.; Dall' Olio, A.; Matsui, E.; Gat, J.R. Recycling of water in the Amazon basin: An isotopic study. *Water Resour. Res.* **1979**, *15*, 1250–1258. [CrossRef]